










REPORT



Sym021, a promising anti-PD1 clinical candidate antibody derived from a new chicken antibody discovery platform

Torben Gjetting ^a, Monika Gad^b, Camilla Fröhlich ^c, Trine Lindsted^b, Maria C Melander^c, Vikram K Bhatia^a, Michael M Grandal ^b, Nikolaj Dietrich ^a, Franziska Uhlenbrock^b, Gunther R Galler^a, Magnus Strandh ^a, Johan Lantto ^d, Thomas Bouquin ^a, Ivan D Horak^d, Michael Kragh^c, Mikkel W Pedersen ^b, and Klaus Koefoed ^a

^aAntibody Discovery, Antibody Discovery, Ballerup, Denmark; ^bCancer Biology and Immunology, Symphogen A/S, Ballerup, Denmark; ^cAntibody Pharmacology, Symphogen A/S, Ballerup, Denmark; ^dGlobal Research and Development, Symphogen A/S, Ballerup, Denmark

ABSTRACT

Discovery of therapeutic antibodies is a field of intense development, where immunization of rodents remains a major source of antibody candidates. However, high orthologue protein sequence homology between human and rodent species disfavors generation of antibodies against functionally conserved binding epitopes. Chickens are phylogenetically distant from mammals. Since chickens generate antibodies from a restricted set of germline genes, the possibility of adapting the Symplex antibody discovery platform to chicken immunoglobulin genes and combining it with high-throughput humanization of antibody frameworks by “mass complementarity-determining region grafting” was explored. Hence, *wild type* chickens were immunized with an immune checkpoint inhibitor programmed cell death 1 (PD1) antigen, and a repertoire of 144 antibodies was generated. The PD1 antibody repertoire was successfully humanized, and we found that most humanized antibodies retained affinity largely similar to that of the parental chicken antibodies. The lead antibody Sym021 blocked PD-L1 and PD-L2 ligand binding, resulting in elevated T-cell cytokine production *in vitro*. Detailed epitope mapping showed that the epitope recognized by Sym021 was unique compared to the clinically approved PD1 antibodies pembrolizumab and nivolumab. Moreover, Sym021 bound human PD1 with a stronger affinity (30 pM) compared to nivolumab and pembrolizumab, while also cross-reacting with cynomolgus and mouse PD1. This enabled direct testing of Sym021 in the syngeneic mouse *in vivo* cancer models and evaluation of preclinical toxicology in cynomolgus monkeys. Preclinical *in vivo* evaluation in various murine and human tumor models demonstrated a pronounced anti-tumor effect of Sym021, supporting its current evaluation in a Phase 1 clinical trial.

Abbreviations: ADCC, antibody-dependent cellular cytotoxicity; CD, cluster of differentiation; CDC, complement-dependent cytotoxicity; CDR, complementarity determining region; DC, dendritic cell; ELISA, enzyme-linked immunosorbent assay; FACS, fluorescence activated cell sorting; FR, framework region; GM-CSF, granulocyte-macrophage colony-stimulating factor; HRP, horseradish peroxidase; IgG, immunoglobulin G; IL, interleukin; IFN, interferon; mAb, monoclonal antibody; MLR, mixed lymphocyte reaction; NK, natural killer; PBMC, peripheral blood mono-nuclear cell; PD1, programmed cell death 1; PDL1, programmed cell death ligand 1; RT-PCR, reverse transcription polymerase chain reaction; SEB, Staphylococcus Enterotoxin B; SPR, surface Plasmon Resonance; VL, variable part of light chain; VH, variable part of heavy chain

ARTICLE HISTORY

Received 23 January 2019
Revised 6 March 2019
Accepted 12 March 2019



KEYWORDS

Chicken antibodies;
antibody repertoire diversity;
immune-oncology; PD1

Introduction

Antibodies have become the most successful among therapeutic proteins across major therapeutic areas like cancer, autoimmune and chronic inflammatory diseases, and they comprise the most rapidly growing drug class.¹ Historically, clinically applied antibodies have been obtained from either hybridoma cloning of B cells from immunized wild-type mice, human transgenic mice or by display technologies like phage display.² The majority of approved therapeutic antibodies are derived from mouse immunizations,^{3,4} indicating that the therapeutic antibody discovery process may be more successful when based on material from immunized animals. The use of animal immunization for antibody discovery requires that the animal can mount a robust antibody response against the antigen, which can be challenging for

proteins or functional epitopes that are highly conserved between species. One solution to overcome this limitation is to use divergent animal species that are evolutionarily more distant to mammals. Chicken (*Gallus gallus*) is one such species, and sequencing of its genome has shown that on an evolutionary scale they separated from humans 300 million years ago.⁵ In comparison, mice separated from humans 88 million years ago, and are consequently phylogenetically more related.⁶ The chicken immunoglobulin system is also distinct from mammals. Whereas human, primate, and rodent immunoglobulin diversity generation is based on the rearrangement of multiple V-, D-, J-gene families, antibody diversification in chickens is based on gene conversion followed by affinity maturation with a fixed set of VH/VL genes.^{7–11}

CONTACT Torben Gjetting  tgj@symphogen.com  Symphogen A/S, Pederstrupvej 93, Ballerup DK-2750, Denmark

 Supplemental data for this article can be accessed on the [publisher's website](#).

© 2019 The Author(s). Published with license by Taylor & Francis Group, LLC.

This is an Open Access article distributed under the terms of the Creative Commons Attribution-NonCommercial-NoDerivatives License (<http://creativecommons.org/licenses/by-nc-nd/4.0/>), which permits non-commercial re-use, distribution, and reproduction in any medium, provided the original work is properly cited, and is not altered, transformed, or built upon in any way.

Chickens may not only be able to raise antibodies against very conserved targets, but also against novel human functional epitopes that are masked in mice due to sequence conservation. Furthermore, antibodies against human targets generated in chicken are often cross-reactive to the mouse orthologous target. Cross-reactivity is important for pre-clinical development of therapeutic antibodies, which often relies on murine models. Here, the potential of using chickens as a species for raising antibodies for therapeutic use was explored by implementing a modified Symplex antibody cloning strategy¹² that could be applied to chicken B cells. The Symplex technology is a PCR-based method for efficient cloning of natively combined variable heavy chain (VH) and variable light chain (VL) gene fragments derived from individual B cells, without VH-VL chain shuffling. In addition, a high-throughput method for humanization of the chicken-derived antibodies was developed, which allowed rapid humanization of the whole antigen-specific antibody repertoire prior to functional screening. The target of choice for the exploratory study was programmed cell death protein 1 (PD1). PD1 is a cell surface receptor that belongs to the immunoglobulin superfamily and is expressed in an inducible manner on mainly CD4⁺ and CD8⁺ T-cells, and pro-B cells.^{13,14} PD1 functions as a co-inhibitory receptor on T-cells and serves as a checkpoint against unrestrained T-cell activation. PD1 plays an important role in maintaining peripheral tolerance as well as immune homeostasis during infection. Tumors can take advantage of this mechanism by upregulating expression of the ligands PDL1 and PDL2, which bind PD1 on effector T-cells, thus inhibiting the anti-tumor immune response mediated by these cells.^{15,16} To date, six therapeutic antibodies targeting the PD1-PDL1/2 pathway, including pembrolizumab (Keytruda) and nivolumab (Opdivo), have been approved in the US and European Union for treatment of various types of cancer.¹⁷ In this study, a large antibody repertoire against PD1 was raised in chickens and subsequently humanized. The resulting humanized antibody panel displayed a very broad epitope coverage, including new and unique functional epitopes conserved between humans and mice. Many of the chicken-derived antibodies had very high binding affinities and showed biophysical properties acceptable for drug development. Detailed functional screening and characterization lead to the identification of a novel anti-PD1 antibody designated Sym021. This antibody bound human PD1 with 30 pM affinity and cross-reacted with both cynomolgus and mouse PD1 with pM affinities, which enabled preclinical *in vivo* studies. Our results show that Sym021 blocks PDL1 and PDL2 ligand binding and demonstrates potent functional activity both *in vitro* and *in vivo*.

Results

Antibody repertoire screening, humanization and sequence analysis

Sequence alignment of human, mouse and chicken PD1 extracellular domains showed that a larger proportion of the surface-exposed residues is shared between human and mouse (60% sequence identity) relative to human and chicken (27% sequence identity), in agreement with the phylogenetic distance between these species (Figure 1(a)). The Symplex RT-

PCR antibody cloning procedure¹² was adapted for chicken immunoglobulin genes, and native pairs of chimeric chicken VH/VL fragments were amplified from single chicken B cells isolated via fluorescence activated cell sorting (FACS) and cloned in-frame with an effector function attenuated human constant IgG1-LALA gene.^{18,19} Full-length chimeric IgG antibodies were expressed transiently in HEK293 cells and screened for binding to mouse and human PD1 antigen by flow cytometry, revealing a large diverse anti-human PD1 antibody repertoire consisting of 144 unique antibodies assigned to 50 different clonal families, so-called clonotypes. The diversity was visualized by sequence clustering in a circular cladogram based on phylogenetic distance²⁰ (Figure 1(b), see details in Supplementary Figure 1). Several intrinsic features of the obtained antibody repertoire were identified. First, in agreement with previous observations,^{8,10,21} we found that the chicken heavy chain complementarity-determining region 3 (CDR3) lengths were considerably longer (average 21 amino acids) than typically found in human (average 16 amino acids) or mouse (average 12 amino acids) antibody repertoires.²² Second, additional putative disulfide bridges were observed in the variable regions. These VH disulfide bridge configurations can be assigned to different canonical types as previously defined¹⁰ (Supplementary Figure 2), and the abundance of each type in the sequenced chicken antibody repertoire is shown in Figure 1(c). Most antibodies were type 1, which has one extra intra-HCDR3 cysteine bridge, or type 2, which has no extra disulfide bridges. A clear correlation between longer HCDR3 length and type 1 configuration was observed (Figure 1(d)) in accordance with previous findings. In addition to the extra disulfide bridges in VH, putative disulfide bridges in VL were also observed, and these resided in both framework regions (FRs) and CDRs. Antibodies with one additional cysteine (free Cys) were deselected from further characterization, since cysteines that do not form disulfide bridges may cause accelerated systemic clearance and are generally not considered compatible with drug development.²³ Likewise, antibodies with extra N-glycosylation sites were deselected,²⁴ resulting in a repertoire of 123 unique antibodies distributed into 46 clonal families. To avoid immunogenicity of chimeric antibodies, a humanization step was performed by grafting the cognate unique chicken CDRs onto human frameworks as previously described for mouse antibodies²⁵ (Supplementary Figure 3). Vernier positions are known to play an important role in antibody structure, stability and function, hence the gene designs also incorporated variation between human and chicken frameworks at selected Vernier residue positions both in VH and VL framework,²⁶⁻²⁸ resulting in the generation of up to four humanization variants for each antibody. Apart from Vernier residue variants, the *in-silico* CDR grafting step did not include variants with mutations in the chicken immunoglobulin frameworks. An overview of the selection and humanization workflow is shown in Supplementary Figure 3A, and the frequency of sequence variations of the antibody repertoire before and after CDR grafting is shown in Supplementary Figure 3B. Antibodies with unique cognate VH/VL CDRs representing the 46 clonal families were grafted *in silico*, and Vernier variants of each unique antibody were

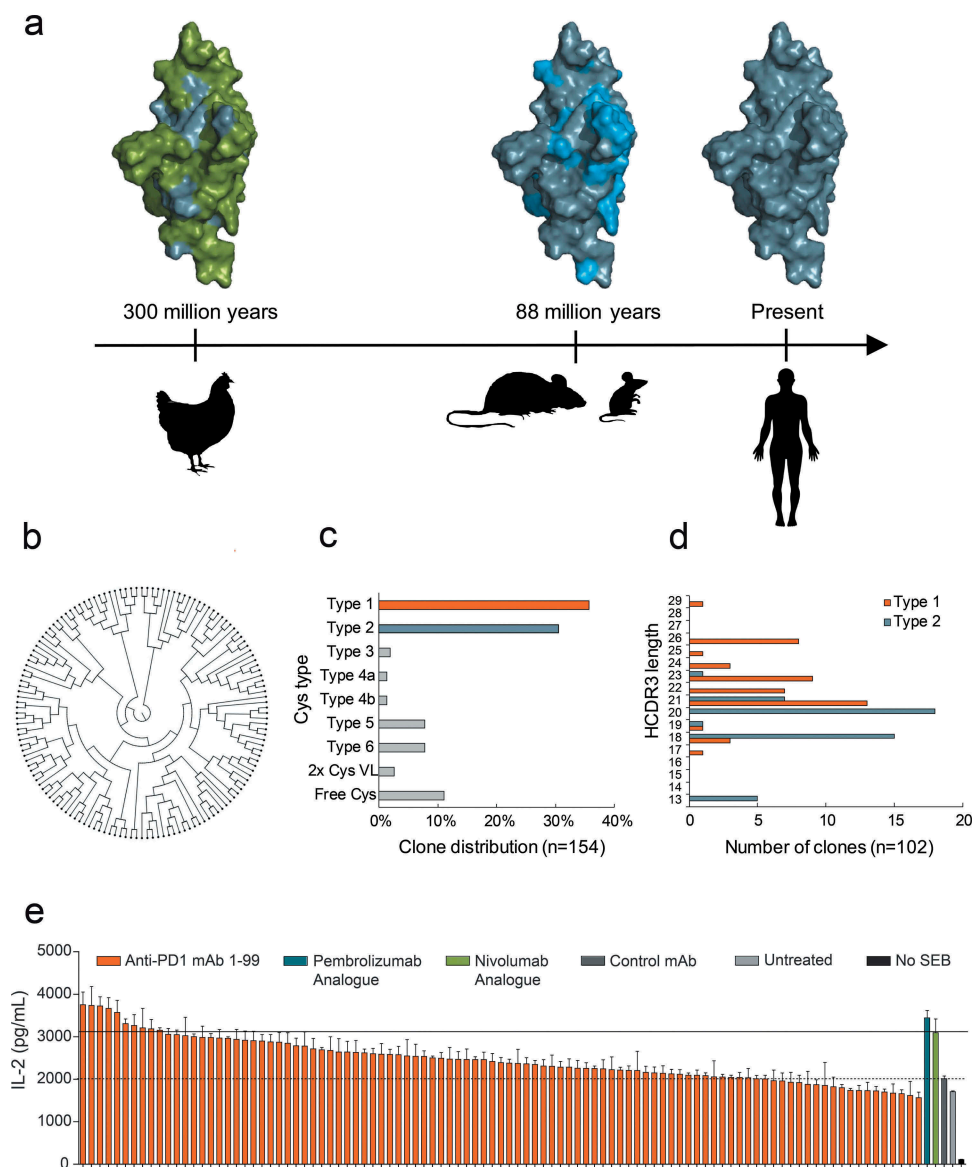


Figure 1. a Amino acid residue differences shown by the coloring of surface-exposed residues in extracellular domain of PD1. Human/common (gray), different in chicken (green), different in mouse (blue). Timeline (arrow) indicates evolutionary time distance since common ancestor.⁶ b ClustalO analysis of 144 chicken-derived antibodies shows high sequence diversity as displayed in a circular cladogram. c Distribution of Cys configuration in repertoire into distinct types as defined previously.¹⁰ d HCDR3 length distribution of antibodies with Cys type 1 (orange) and type 2 (blue) configuration. e Waterfall plot showing a ranking of 99 humanized anti-PD1 antibodies tested for functional activity in an SEB whole blood assay at 1 μ g/ml. Analogue of pembrolizumab and nivolumab were included as a positive control, and the negative control mAb was a human IgG1 LALA that binds to an irrelevant non-human antigen. IL-2 levels in the supernatants were determined after 48 h of culture. Horizontal lines indicate IL-2 levels after treatment with control mAb (dashed) or nivolumab analogue (solid). Each bar represents mean \pm SEM (n = 3).

generated. Genes were generated by *de novo* gene fragment synthesis and used for cloning and expression of full-length humanized IgG1-LALA antibodies. Flow cytometry and enzyme-linked immunosorbent assay (ELISA) analyses were used to confirm PD1 binding, and, of the original 46 clonotypes used for CDR grafting, 34 clonotypes were successfully humanized, corresponding to a humanization success of 74%. Figure 1(e) shows the functional screening of 99 humanized antibodies that were evaluated for efficacy in a superantigen (SEB) whole blood stimulation assay using interleukin (IL)-2 secretion as a read-out. Several antibody candidates were selected for further analysis based on this functional readout, and the six top-ranking antibodies were produced in higher

amounts for further functional testing. An additional antibody, mAb7, was included in the functional evaluation because it exhibited activity in the SEB assay but did not efficiently block PD1 ligands PD-L1 and PD-L2.

Characterization of humanized chicken antibodies

The seven selected humanized chicken-derived antibodies were evaluated for PD1 binding affinity and functional activity and compared directly to the reference antibodies pembrolizumab and nivolumab (Table 1). The monomeric binding was measured by surface plasmon resonance (SPR) biosensor analysis using

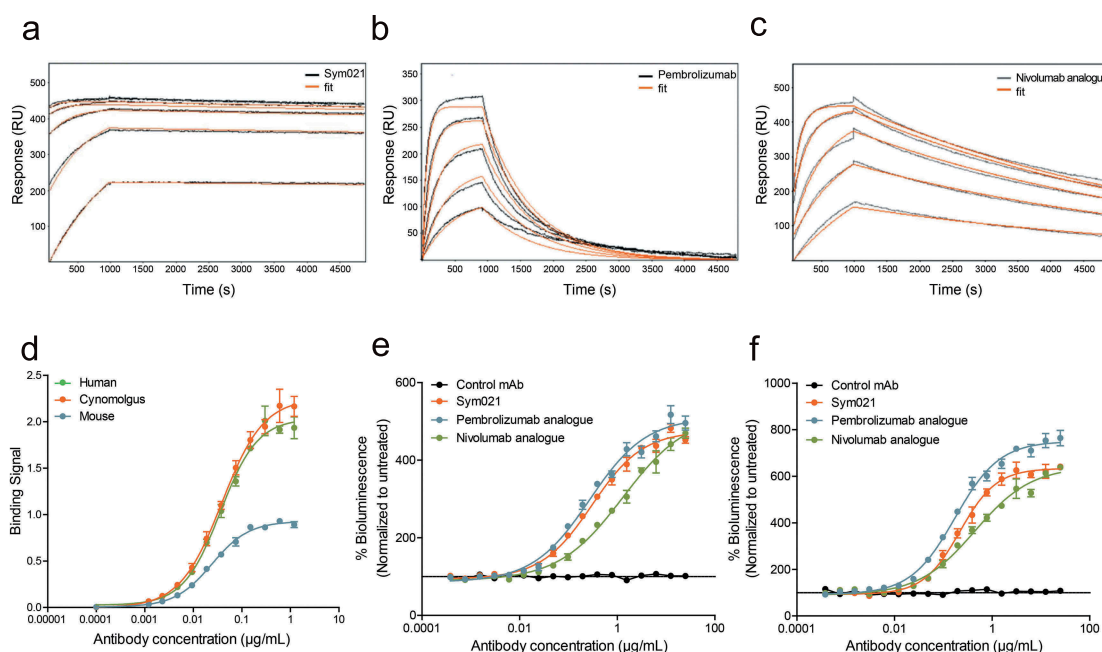


Figure 2. Surface plasmon resonance (SPR) sensorgrams and fits of the binding kinetics of a Sym021, b pembrolizumab and c nivolumab analogue binding monomeric human PD1. d Binding of Sym021 to human, cynomolgus and mouse PD1 as determined by ELISA. Data points are shown as mean values \pm SD of duplicates. Dose–response curves for Sym021 in cell-based e PD-L1 blocking assay and f PD-L2 blocking assay. Analogues of pembrolizumab and nivolumab were included as a positive control, and the negative control mAb was a human IgG1 LALA that binds to an irrelevant non-human antigen. Data are presented as percent increase in luciferase signal upon blocking. Each datapoint represents mean \pm SEM.

kinetic titration of recombinant antigens. All tested humanized antibodies recognized human PD1 with high picomolar affinities and showed strong cross-reactivity with cynomolgus PD1. The three antibodies with the highest affinity for human PD1 contained HCDR3s with two extra cysteines (type 1). Mab1 (henceforth called Sym021) was the clone with the highest affinity of all tested antibodies and bound human PD1 with a monovalent affinity of 30 pM, while nivolumab and pembrolizumab bound with affinities of 800 pM and 2800 pM, respectively (Figure 2(a-c) and Table 1). Both the purchased pembrolizumab and the pembrolizumab analogue showed similar kinetic properties, thereby confirming our analogue design. While both Sym021, nivolumab, and pembrolizumab showed comparable on-rates, the significantly stronger affinity of Sym021 stemmed from a \sim 20- to \sim 150-fold slower dissociation constant (off-rate), clearly visible in the sensorgram (Figure 2(a-c)). Importantly, Sym021 was the only antibody found to be cross-reactive with both cynomolgus monkey and mouse PD1, with strong binding affinities of 110 pM and 810 pM, respectively, whereas nivolumab and pembrolizumab only bound cynomolgus monkey PD1 with affinities of 1500 pM and 3600 pM, respectively (Table 1). The potent binding of Sym021 to all three species was confirmed by ELISA using recombinant antigens (Figure 2(d)). The panel of humanized chicken-derived antibodies was evaluated for blocking the interaction of PD1 with its ligands PD-L1 or -L2, and the ability to promote a T-cell induced IL-2 response *in vitro* in a whole blood SEB stimulation assay (Table 1). All antibodies except mAb7 showed efficient blocking of PD-L1/L2 ligand binding and were found to be highly functional in the SEB assay. Although mAb7 did not efficiently block PD1 ligands, it did exhibit some activity in the SEB assay, suggesting it was interfering with PD1 signaling via

a different mechanism of action. Overall, Sym021 was the most potent humanized antibody in the SEB assay, and when tested in cellular PD1/PD-L1 or PD1/PD-L2 reporter assays, Sym021 blocked the PD1/PD-L1 and PD1/PD-L2 interactions to a similar degree as nivolumab and pembrolizumab (Figure 2(e-f)).

Epitope mapping of functional humanized antibodies

The functional humanized chicken-derived antibodies Sym021, mAb2, and mAb7 were subjected to detailed epitope mapping to further explore the mechanism(s) of action, and to assess if the epitopes were different from the clinically approved nivolumab and pembrolizumab. All five antibodies were mapped in high resolution by analyzing the binding affinity to 111 mutated PD1 variants in which surface-exposed amino acids were substituted with alanine (alanine scanning), or linear segments of 10 amino acids in the human PD1 sequence exchanged sequentially to the corresponding chicken PD1 sequence (linear epitope mapping). The analysis showed that the binding epitopes of Sym021, mAb2 and mAb7 were distinct from the binding epitopes of the reference antibodies nivolumab and pembrolizumab^{29,30} (Figure 3 and Supplementary Table 1). All tested antibodies except mAb7 were found to overlap with the PD-L1 binding site, consistent with their high functional activity and ligand blocking properties (Table 1). Alanine scanning mapped the epitope of mAb7 to residues V44 and T145 that clustered to the stem of PD1, distant to the PD-L1 binding site (Figure 3) consistent with a strong binding affinity of 60 pM, but only partial PD-L1 and PD-L2 blocking activity observed for this antibody. The most functional humanized chicken-derived antibodies Sym021 and mAb2, together with nivolumab and pembrolizumab, bound to overlapping epitopes

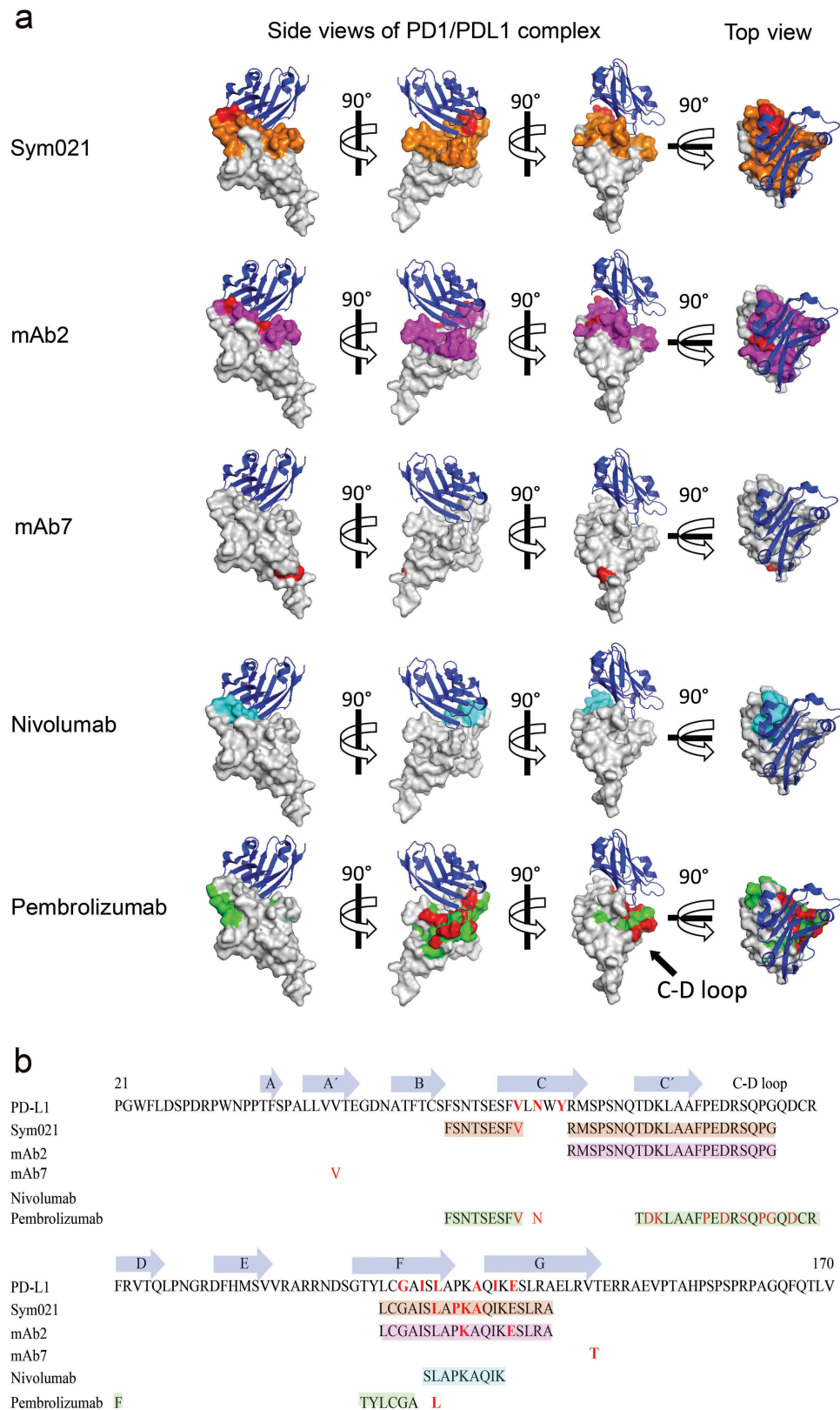


Figure 3. Epitope mapping of PD1 antibodies. **a** Epitope of Sym021 relative to humanized chicken-derived antibodies mAb2, mAb7 and reference antibodies nivolumab and pembrolizumab is imposed on a space filling model of human PD1 (overlay of 4ZQK and 2M2D structures). Three side views of the PD1-PD-L1 complex rotated 90° apart are displayed together with a top view of the PD-L1 ligand binding surface. Blue: PD-L1 ligand in cartoon, Gray: Space-filling model of PD1. Red: Contact residues identified by alanine scanning. Orange: Linear epitopes for Sym021. Magenta: Linear epitopes for mAb2, Cyan: Linear epitopes for nivolumab. Green: Linear epitopes for pembrolizumab. **b** The PD1 amino acid sequence with annotated β -strands, linear epitopes, and contact residues are shown for PD-L1 and epitope mapped antibodies. The β -strand definitions were based on Lin *et al.*²⁹ and Zak *et al.*³⁰

Table 1. Functional characteristics of humanized anti-PD1 antibodies. Binding kinetics (on-rate, off-rate, KD) to human, cynomolgus or mouse PD1 was measured by SPR. PD-L1 or PD-L2 blocking assays were performed by Biolayer Interferometry analysis. Cell-based functionality was evaluated by the SEB whole blood assay using IL-2 as readout. Max SEB and EC50 SEB represent the maximal efficacy of IL-2 stimulation and the potency in the SEB assay, respectively. HCDR3 length and Cys type¹⁰ are indicated.

Antibody	PD1	$k_{on}(M^{-1} s^{-1})$	$k_{off}(s^{-1})$	KD (pM)	PD-L1block	PD-L2block	Max SEB(pg/ml IL-2)	EC50SEB (nM)	HCDR3Length	Cys type
mAb1 (Sym021)	Human	3.3×10^5	8.9×10^{-06}	30	Yes	Yes	3738	122	19	1
	Cynomolgus	1.1×10^5	1.2×10^{-05}	110						
	Mouse	3.7×10^4	3.0×10^{-05}	810						
mAb2	Human	4.2×10^5	2.3×10^{-04}	560	Yes	Yes	3572	356	21	1
	Cynomolgus	5.1×10^5	3.8×10^{-04}	740						
mAb3	Human	1.4×10^6	6.3×10^{-05}	50	Yes	Yes	3057	177	23	1
	Cynomolgus	2.5×10^6	6.1×10^{-04}	250						
mAb4	Human	4.6×10^5	3.4×10^{-04}	740	Yes	Yes	2370	390	18	2
	Cynomolgus	2.9×10^5	6.9×10^{-04}	2340						
mAb5	Human	7.1×10^5	3.8×10^{-04}	340	Yes	Yes	2938	457	18	2
	Cynomolgus	3.2×10^5	7.0×10^{-04}	2220						
mAb6	Human	2.4×10^5	7.2×10^{-03}	540	Yes	Yes	3308	691	21	2
	Cynomolgus	1.0×10^6	1.7×10^{-04}	680						
mAb7	Human	1.2×10^6	6.9×10^{-05}	60	Partial	Partial	2639	920	24	1
	Cynomolgus	2.5×10^6	1.1×10^{-03}	450						
Nivolumab analogue	Human	2.4×10^5	1.9×10^{-04}	800	Yes	Yes	3094	498	8	2
	Cynomolgus	4.1×10^5	6.2×10^{-04}	1500						
Pembrolizumab analogue	Human	4.8×10^5	1.3×10^{-03}	2800	Yes	Yes	3445	40	15	2
	Cynomolgus	4.0×10^5	1.4×10^{-03}	3570						
Pembrolizumab (Keytruda®)	Human	4.2×10^5	1.4×10^{-03}	3360	Yes	Yes	N.D.	N.D.	15	2
	Cynomolgus	3.5×10^5	1.3×10^{-03}	3630						

that fully or partially covered the PD-L1 binding site (Figure 3(a)). More specifically, parts of the Sym021 and pembrolizumab epitopes were mapped to a linear PD1 segment defined by amino acids 56–64 partially overlapping with the C β -strand, consistent with sensitivity for the V64 single mutant (Figure 3 and Supplementary Table 1). The C β -strand also contains three contact residues for PD-L1. Furthermore, both Sym021 and mAb2 were mapped to linear amino acid segment 69–90 overlapping with the C' β -strand, while pembrolizumab bound the more distal linear epitope located on the side of PD1 defined by amino acid segments 76–95. Alanine scanning revealed that binding of pembrolizumab was mainly dependent on residues located in the C-D loop consistent with previous X-ray structure analysis.³¹ The core epitopes of Sym021 and mAb2 were shown by alanine scanning and linear epitope mapping to be located in amino acid segment 122–140, while nivolumab was found to bind to a smaller linear epitope defined by amino acids 127–135, both overlapping with the F and G β -strands of PD1. Pembrolizumab also bound to a smaller linear epitope defined by amino acids 120–125 located in the F β -strand. The F and G β -strands also contains six contact residues for human PD-L1 (Figure 3, Supplementary Table 1).

In summary, the epitope mapping data indicated that all antibodies except mAb7 bind distinct epitopes that overlap with the PD-L1 binding site, consistent with the PD-L1 ligand blocking data. Sym021 was the only antibody in the investigated anti-PD1 panel that cross-reacted with mouse PD1 (KD 810 pM), further supporting that the binding epitope of this antibody is unique compared to the other tested PD1 antibodies. Since Sym021 was also the most potent and efficacious humanized chicken-derived antibody in terms of binding affinity and functional activity, it constituted a potential drug lead and was thus subjected to further characterization *in vitro* and *in vivo*.

Sym021 *in vitro* functionality

The ability of Sym021 to promote a T cell response *in vitro* was assessed by full titration in a whole blood SEB

stimulation assay. As shown in Figure 4(a), treatment with Sym021 enhanced the SEB-induced T cell response, leading to a dose-dependent increase in IL-2 secretion. The observed activity of Sym021 was comparable to the activity of the pembrolizumab analogue. *In vitro* functional activity of Sym021 was further validated in an allogeneic mixed lymphocyte reaction (MLR) assay using human monocyte-derived dendritic cells (DC) and CD4⁺ T cells. In this assay, blockade of PD1 by Sym021 potently induced interferon (IFN)- γ secretion in a dose-dependent manner. Results from a representative DC/T cell donor pair is shown in Figure 4(b). Importantly, Sym021 showed activity in a large panel of independent DC/T cell donor pairs in MLR assays. Although the magnitude of the response varied between individual donor pairs, Sym021 induced a statistically significant increase in IFN- γ secretion in all 16 donor pairs compared to the negative control antibody ($p < 0.001$) (Figure 4(c)). CD4⁺ T cells derived from the MLR experiments were further analyzed with respect to T cell activation, proliferation and cytokine release upon treatment with Sym021 by flow cytometry. As shown in Figure 4(d), CD4⁺ T cells treated with Sym021 expressed higher levels of CD25, indicative of T cell activation. Moreover, T cell proliferation (Ki-67) and the secretion of IFN- γ were significantly increased compared to treatment with control antibodies ($p < 0.001$ and $p < 0.001$, respectively).

As mentioned earlier, a key feature of the chicken-derived Sym021 antibody is the cross-reactivity not only to cynomolgus PD1 but also to mouse PD1. Functional activity in murine cells is advantageous because it allows for preclinical evaluation of Sym021 in murine syngeneic *in vivo* models. Demonstration of cross-species functional activity was carried out *in vitro* using SEB stimulation of either human peripheral blood mononuclear cells (PBMCs), cynomolgus PBMCs or murine spleen cells. As shown in Figure 4(e), the activity of Sym021 in cynomolgus and mouse cells was comparable to that observed using human cells, as treatment with Sym021 induced a similar dose-dependent increase in IL-2 secretion in all three species.

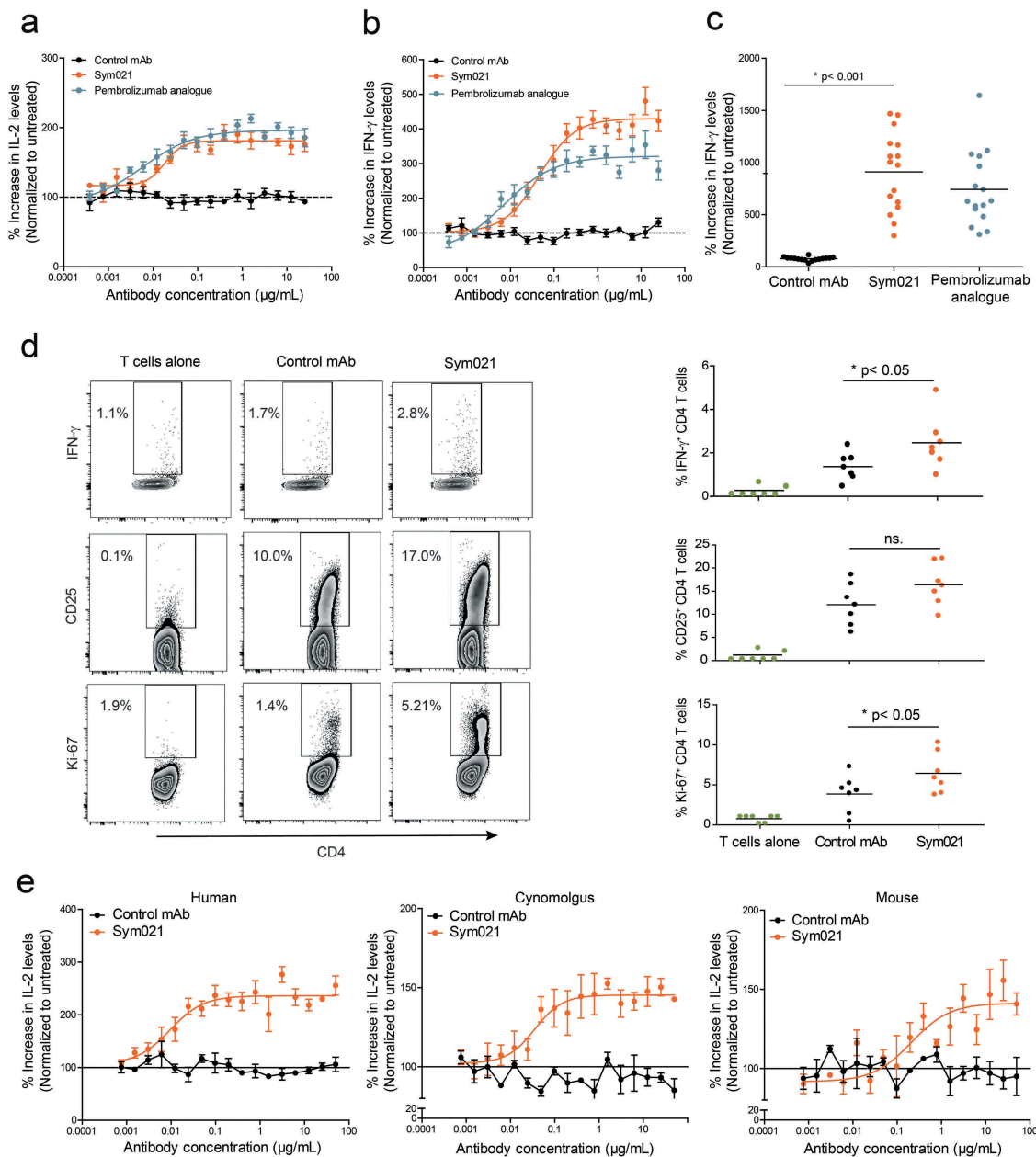


Figure 4. Dose–response curve of Sym021 in a SEB whole blood assay and in b one-way MLR assay. An analogue of pembrolizumab was included as a positive control, and the negative control mAb was a human IgG1 LALA that binds to an irrelevant non-human antigen IL-2 and IFN- γ levels in the supernatants were determined by ELISA after 48 h and 5 days of culture, respectively. Data are presented as percent increase in cytokine levels relative to untreated. Each datapoint represents mean \pm SEM (n = 3). c Effect of Sym021 at a single dose (10 µg/mL) in the one-way MLR assay in a panel of 16 independent donor pairs. Data are presented as percent increase in cytokine levels relative to untreated. Each dot represents a donor pair, and the horizontal bar is the mean. d CD4⁺ T cells of seven independent donor pairs from one-way MLR experiments (untreated, negative control mAb, Sym021) were investigated by flow cytometry for the expression of IFN- γ , Ki-67, and CD25 after 48 h of co-culture. Dot plots of one representative donor are depicted (left). The increase of T cell-stimulatory effects induced by Sym021 is depicted on the right. Each dot represents an individual donor, and the horizontal bar is the mean. e Dose–response curves of Sym021 in either human PBMCs, cynomolgus PBMCs or murine (C57B1/6J) spleen cells stimulated with SEB. IL-2 levels in the supernatants were determined by ELISA after 48 h of culture. Data are presented as percent increase in cytokine levels relative to untreated. Each datapoint represents mean \pm SEM (n = 3). * p < 0.05, ** p < 0.01, ***p < 0.001, ****p < 0.0001.

We confirmed that Sym021, as an IgG1 LALA effector antibody, does not possess any measurable ADCC or CDC activity *in vitro* (Supplementary Figure 4).

In summary, Sym021 potently enhances T cell responses and cytokine production in *in vitro* functional assays using human and cynomolgus, as well as murine primary cells.

Sym021 inhibits tumor growth in murine and human tumor models

The capability of Sym021 to activate T cells was explored *in vivo* using various tumor models. Sym021 was initially tested in four murine syngeneic tumor models. In the Sa1N (fibrosarcoma) syngeneic tumor model, Sym021 showed a pronounced effect on tumor growth with complete

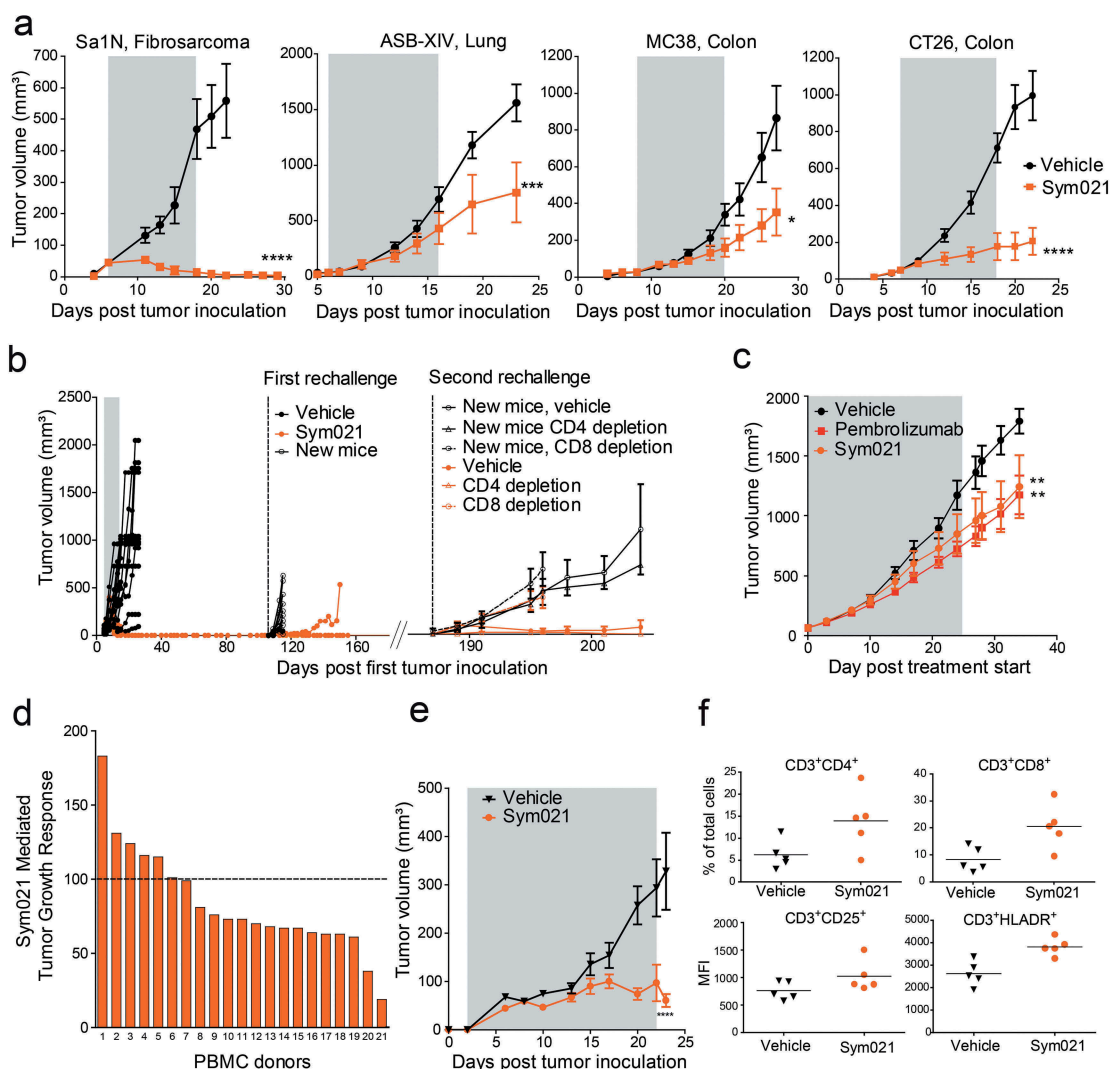


Figure 5. a Growth of Sa1N, CT26, ASB-XIV, or MC38 syngeneic tumors was measured in mice during and for a period following injections of vehicle buffer or Sym021 (10 mg/kg); n = 10 mice/group. The gray area denotes the treatment period. b Growth of ASB-XIV syngeneic tumors. Left part of the graph: Mice were dosed with vehicle buffer (n = 12) or Sym021 (10 mg/kg) (n = 14). The gray area denotes the treatment period. First rechallenge: mice with eradicated tumors in the Sym021 treated group (n = 14) and 10 new BALB/c mice were s.c. inoculated with ASB-XIV cells into the opposite flank. Right part of the graph: In the second rechallenge, 12 of the surviving mice in the Sym021 treated group and 10 new control BALB/c mice were s.c. inoculated with ASB-XIV cells into the opposite flank from the first rechallenge. Two days prior to tumor inoculation and hereafter twice weekly, mice received vehicle buffer or either CD4 or CD8 depletion antibody. c CD34⁺ humanized NSG-SGM3 mice engrafted with human lung PDX model and treated with vehicle, Sym021 or pembrolizumab. d Growth of A375 xenograft in PBMC humanized mice. One human PBMC donor was used per study. Treatment was initiated at the day of PBMC injection and mice were treated as described in (A). The waterfall plot shows the percentage of tumor growth inhibition at the end of the study. (D). The gray area denotes the treatment period. e Tumor growth in mice reconstituted with PBMCs from donor 21 from (D). The gray area denotes the treatment period. f Flow cytometric analysis of tumor-infiltrating lymphocytes from donor 21. Percent of total CD3⁺CD4⁺ (upper left) and CD3⁺CD8⁺ (upper right) T cells and CD25 (lower left) and HLA-DR (lower right) expression on CD3⁺ cells in Sym021 treated tumors compared to vehicle. Data are presented as means ± SEM. * p < 0.05, ** p < 0.01, ***p < 0.001, ****p < 0.0001.

eradication of all treated tumors (Figure 5(a)). In the other three models, Sym021 treatment showed overall tumor growth inhibition, with some responding and non-responding mice present in each model. No body weight loss or adverse effects were observed in any of the models upon treatment (data not shown). Sym021 treatment did not result in an anti-tumor effect in immunodeficient CT26 engrafted SCID mice, which lack T cells (the Sym021 target cells) but retain functional natural killer cells, demonstrating that a functioning immune system is required for Sym021 *in vivo* activity (Supplementary Figure 5). To further investigate the mechanism behind the tumor growth inhibitory

activity of Sym021, 14 mice with Sym021 eradicated ASB-XIV syngeneic tumors were rechallenged with a new inoculation of ASB-XIV tumor cells (Figure 5(b), left graph). In 13 of the rechallenged mice, no tumor growth was observed, suggesting induction of an immune memory response. To investigate whether T cells were responsible for rejecting tumor growth, CD8⁺ and CD4⁺ cells were depleted prior to and during the second rechallenge of ASB-XIV tumor cells (Figure 5(b), right graph). Depletion of CD8⁺ T cells in the mice allowed tumor growth in the rechallenged mice comparable to control mice receiving CD8 depleting antibodies. In contrast, no

tumor growth was observed in rechallenged mice with depletion of CD4⁺ T cells. These data indicate that in tumor rechallenged mice, CD8⁺ T cells are the primary cells driving the Sym021-mediated anti-tumor effect.

The *in vivo* antitumor effect of Sym021 was compared to that of pembrolizumab in CD34⁺ humanized NSG-SGM3 mice engrafted with a human lung PDX model. As shown in Figure 5(c), the results demonstrated an equivalent anti-tumor effect of Sym021 and pembrolizumab in the PDX model. The tumor growth was significantly delayed compared to vehicle treated tumors (Figure 5(c)). To further explore the anti-tumor effect of Sym021 in human tumor models, Sym021 was tested in mice reconstituted with human PBMCs and engrafted with the human melanoma A375 tumor xenograft model. One healthy human PBMC donor was used in each experiment and the efficacy of Sym021 was evaluated with PBMCs from 21 different donors. Sym021 induced a tumor growth inhibitory response in 67% (14 of 21 donors) of the tested donors (Figure 5(d)). A pronounced effect, with almost no gain in tumor size during treatment, was observed in donor 21 (Figure 5(d-e)). In the responding models, Sym021 increased the number of tumor-infiltrating CD8⁺ and CD4⁺ T cells, which displayed a more activated phenotype as demonstrated by increased expression of CD25 and HLA-DR on CD3⁺ cells (Figure 5(f)).

In summary, *in vivo* data demonstrated that Sym021 induces activation of immune cells, primarily CD8⁺ T cells, and results in potent *in vivo* efficacy in various mouse models of murine and human cancer as measured by tumor growth inhibition.

Discussion

Faithful representation of the interplay between the host immune system and the tumor microenvironment is essential for modeling therapeutic antibody activity of immune-oncology drugs *in vivo*. Hence, orthologue target cross-reactivity of an antibody lead molecule in species used for *in vivo* efficacy and toxicity modeling (e.g. mice, cynomolgus monkey) is a desirable feature to validate biological rationale. From a phylogenetic perspective, the chicken is an attractive species for generating antibodies against human targets that are highly conserved and non-immunogenic in mammals. Furthermore, chicken antibodies raised against a human target often cross-react with orthologous targets from species such as cynomolgus monkeys and mice,^{11,32-34} PD1 is a well-known immune checkpoint target, and it has previously been difficult to obtain therapeutic drug candidates that cross-react to mouse PD1 with a high enough affinity to mediate functional activity in syngeneic mouse models.³⁵

Using PD1 as an example, we developed a novel therapeutic antibody discovery platform based on immunization of wild type chickens to obtain differentiated functional antibodies that cross-react with orthologous mouse and cynomolgus monkey PD1 with high affinity. Previously used methods for cloning of chicken antibodies have been based on phage display of combinatorial VH and VL libraries^{10,34,36,37} or direct B-cell screening and cloning.^{21,38} However, both methods require time-consuming reformatting to a final therapeutic format such as IgG1, that may result in clone attrition.

Furthermore, the inherent shuffling of VH/VL chains by phage display libraries can later manifest in the isolation of clones with reduced binding affinity or specificity,^{39,40} or result in reduced clonal diversity that is skewed towards promiscuous heavy chains combining with different light chains.¹² Consequently, we developed a modified Symplex cloning strategy where natively paired VH/VL chains from single sorted chicken B-cells are directly cloned by RT-PCR and expressed in the final therapeutic IgG format for screening. Finally, to obtain humanized antibodies that can be evaluated in the clinic, we developed a simple, fast and efficient procedure that allows functional testing of entire humanized antibody repertoires, to avoid spending time on single clones that are either difficult to humanize or have inherent stability issues due to the humanization process.

A diverse panel of 144 PD1-specific chimeric chicken-derived antibodies was isolated in this study. The frequencies of the different structural HCDR cysteine types 1 to 6 (Figure 1(c)) were similar to the frequencies identified from sequence analysis of a large data set of 1269 naïve chicken VH sequences,¹⁰ demonstrating that the Symplex procedure enables capture and recovery of the natural unbiased antigen-specific antibody repertoire developed in wild-type chickens.

The anti-PD1 antibodies with an extra HCDR3 disulfide bridge had significantly longer HCDR3s (Figure 1(d)) in agreement with previously published work.^{10,21} Longer CDR3 loops can help antibodies bind to targets in novel ways and may be better at forming deep-reaching, cavity-binding paratopes such as observed for HIV neutralizing antibodies that block CD4,^{41,42} or antibodies that bind membrane transporter proteins with little extracellular protrusion.³⁴

It is desirable for therapeutic antibody candidates to be of fully human origin or undergo a humanization step to avoid immunogenicity. Since chickens diversify antibody sequences using only one set of functional VH and VL V-genes, which are optimized through gene conversion with immunoglobulin pseudogenes, it was envisioned that “mass CDR grafting” of chicken CDRs onto human FRs was possible. Humanization based on the frameworks of the most homologous human germlines IGHV3-23 and IGLV3-19 was used in combination with sequence variation at selected Vernier residues.²⁶⁻²⁸ With this approach, variation in the chicken FRs was not carried forward, but binding specificities encoded by CDRs were successfully grafted onto human FRs by means of *de novo* gene synthesis (Supplementary Figure 3). The simple one-step “mass CDR grafting” procedure obviates the need for time-consuming iterative optimization cycles and structure-based homology modeling, which are usually used in, for example, mouse humanization campaigns. Subsequent analysis revealed that 74% of the clonotypes retained PD1 binding after humanization. The success rate was in line with two other chicken antibody humanization campaigns, where we found that 67% and 86% of the clonotypes retained binding after humanization, respectively (unpublished data). Importantly, very high picomolar PD1 affinities and functional activity were identified in a panel of seven humanized antibodies selected for further studies. The affinities were obtained without any affinity optimization, and the Sym021 affinity was significantly higher than what has been

achieved from the mouse immunizations that resulted in the generation of nivolumab and pembrolizumab.

The epitopes of three humanized chicken-derived antibodies were shown to be distinct compared to nivolumab and pembrolizumab. MAb7 recognized a completely different functional epitope distant from the PD-L1 and PD-L2 binding site that may interfere with PD1 signaling via an allosteric mechanism that is not dependent on PD1 ligand blocking. In contrast, the most potent antibodies Sym021 and mAb2 were found to block both PD1 ligands and overlap with their binding site on PD1. Our findings confirm that chicken immunization can yield antibodies against different functional epitopes, as compared to those resulting from typical mouse immunizations. The epitope of Sym021 was particularly interesting since it allowed for exceptionally strong cross-reactivity to both human, cynomolgus monkey, and mouse PD1.

Moreover, Sym021 shows potent PD-L1 and PD-L2 blocking activity in reporter cell assays and was at least as efficient as nivolumab and pembrolizumab reference antibodies in enhancing T cell responses and cytokine production *in vitro*. In CD34⁺ humanized NSG-SGM3 mice engrafted with human patient-derived lung tumors, Sym021 and pembrolizumab showed equivalent anti-tumor activity despite the higher affinity of Sym021. The study was performed with a high dose level, which should lead to full PD1 target saturation of both pembrolizumab and Sym021.^{43,44} It is therefore highly unlikely that a potential difference in potency between Sym021 and pembrolizumab due to differences in affinity would be evident in the study. To explore if the higher affinity of Sym021 compared to pembrolizumab will provide enhanced anti-tumor activity, more extensive comparisons of the two agents, including multiple dose levels in multiple models, are required. However, other factors such as the different epitopes and isotypes of the two agents may be just as important as affinity at defining the biological activity.

Sym021 cross-reacts with high affinity to mouse PD1, and this enabled testing of the anti-tumor effect in syngeneic tumor models in immunocompetent mice. Sym021 treatment was found to induce significant tumor growth inhibition in several syngeneic tumor models and even complete tumor eradication in the Sa1N mouse fibrosarcoma model. Analysis of the tumor models has shown that the response to Sym021 treatment correlates with immune cell infiltration with the Sa1N model having the highest number of infiltrating T cells (data not shown). Additionally, treatment with Sym021 in a PBMC reconstituted mouse model engrafted with human melanoma tumor cells showed a positive tumor response with PBMCs derived from 67% of the donors. This was accompanied by increased tumor infiltration and enhanced activation of lymphocytes in the responding donor PBMCs, suggesting that Sym021 is highly potent in promoting human T cell activation.

The HCDR3 loop of Sym021 contains two extra cysteines (type 1). During the development of Sym021, we addressed the intra-HCDR3 disulfide bridge stability, and we were able to confirm that it is stable over time and does not contribute to heterogeneity in terms of disulfide scrambling with other structural cysteine bridges (unpublished data). We also observed normal expression level and stability (low

aggregation), similar to fully human antibodies in clinical development. Approximately 6% of the human antibody sequences naturally have HCDR3 sequences with a potential intra-HCDR3 disulfide bridge,⁴⁵ derived from the VDJ recombination with one of four IGHD2 genes (IGHD2-2, IGHD2-8, IGHD2-15, IGHD2-21) that contain two extra cysteines. Such intra-HCDR3 disulfide bridges were also identified in antigen-specific antibodies isolated by the Symplex technology from vaccinia immunized human donors, demonstrating that they are used in natural human antibody repertoires.⁴⁶ Hence, HCDR3s with an additional intra disulfide bridge is a rare but a natural feature of human immune antibody repertoires and can be found in monoclonal antibodies isolated from humans.

Recently, a transgenic chicken with humanized variable region immunoglobulin genes and chicken constant regions was used for the isolation of 41 unique antibodies binding human progranulin.³⁸ We note that, although the requirement for humanization is bypassed, the chicken was engineered with a human kappa VK3-15 light chain that shows only 45% sequence identity to the original *wild type* chicken VL. Replacing the *wild type* chicken VL with human VK3-15 could cause instability of the resulting chimeric antibodies and may explain the lower IgY serum levels observed in the transgenic chicken.³⁸ We used the more homologous IGLV3-19 (65% sequence identity) and did not observe any increased protein aggregation or poor expression of the humanized antibodies. It is of note that, although a high cloning efficiency of 50% was obtained by RT-PCR in our study, the hit rate was still modest when using chicken spleen as a B-cell source (0.1%), especially considering that the immunization was performed with purified human/mouse PD1 protein that is very distant from chicken PD1 in sequence. It is possible that further optimization of immunization procedures, timing of B-cell harvest, use of novel B-cell markers, or other B-cell rich tissue could increase the hit rate considerably. Finally, novel technological advancements, such as next-generation-sequencing and ultra-high through-put microdroplet processing and screening,⁴⁷⁻⁵¹ hold promise for providing more functional antibodies against ever more difficult and conserved targets in immune-oncology.

In summary, the adaptation of the Symplex technology and a one-step humanization procedure for cloning of humanized chicken-derived therapeutic antibody drug candidates proved to be highly efficient. With the exemplary PD1 immunization campaign described here, we demonstrated that we can obtain a diverse antibody repertoire with picomolar affinity, functional antibodies with distinct binding epitopes and a lead antibody with high cross-reactivity to both murine and cynomolgus monkey PD1 that allows for direct evaluation in preclinical *in vivo* models.

Based on these promising results, Sym021 was subjected to non-clinical toxicology studies in cynomolgus monkeys and has since then progressed into a clinical study (NCT03311412) for evaluation of the potential as a therapeutic drug. This is to the best of our knowledge the first study in humans of a chicken-derived therapeutic antibody. Antibodies targeting the PD1/PD-L1 pathway serves as the backbone in many ongoing clinical combination trials,

and the unique features of Sym021 may allow for effective development of novel therapeutic combinations for the treatment of various types of cancers.

Materials and methods

Antibody repertoire generation

Immunization. Wild-type chickens (female, Isa Warren) were used for immunizations with Fc-fusion or his-tagged PD1 extracellular domain (Sino Biologicals). To increase the probability of obtaining antibodies cross-reacting with mouse PD1, a total of seven injections over 2 months were used alternating between human and mouse protein. **Cell sorting.** Cells were harvested from spleen and bone marrow and stained with a combination of fluorescently labeled antibodies against B cell markers to allow for isolation of antibody secreting cells (ASC). ASC were sorted into 384-well microtiter plates containing 1x RT-PCR buffer using a cell sorter (Becton Dickinson FACS Aria I). **RT-PCR/cloning.** Cognate pairs of VH and VL isolated from each ASC were amplified using the Symplex technology^{12,52} and cloned into an expression vector for construction of an expression library of full-length chicken-human chimeric IgG antibodies. The library was expressed by transfection of EXPI-293 cells. **Primary screening.** Primary screening of expression supernatants by flow cytometry in a high-throughput format (iQue® Screener, IntelliCyt) utilized CHO-S cells transiently transfected with human-PD1 to identify anti-PD1 reactive antibodies. **Sequencing.** The chicken VH/VL domains of the retrieved hits were subsequently subjected to DNA sequencing and information about the CDRs was extracted using a hidden Markov model algorithm,⁵³ and this allowed for clonotype clustering as described previously.⁵⁴ The antibody sequence diversity was displayed by concatenating VH/VL protein sequences of each antibody and subjecting it to Clustal Omega clustering.²⁰ **Humanization.** Humanization of the chicken-derived anti-PD1 antibodies was performed using the “CDR grafting” approach, a method originally described by Jones *et al.*²⁵ Briefly, using a Blast algorithm, VH and VL chicken antibody sequences were found to have the closest sequence homology to human germline V and J-genes IGHV3-23/IGHJ1 and IGLV3-19/IGLJ6 that were used for CDR grafting. Several humanized variants were made from each chicken antibody sequence based on different Vernier residue combinations.²⁶ New antibody gene sequences combining chicken CDRs with human FRs were constructed using *de novo* gene fragment synthesis (Genscript) (Supplementary Figure 3). Cognate VH and VL fragments were cloned into an expression vector in-frame with the corresponding constant parts of human immunoglobulin genes, i.e., the lambda constant cDNA fragment for VL and a variant of IgG1 constant region cDNA designated IgG1-LALA for VH. This isotype format refers to heavy chain amino acid residues L234 and L235 (IMGT Eu numbering system⁵⁵) that were mutated into alanine residues, as this has been shown to attenuate complement C1q binding and effector functions mediated through Fc-gamma receptors.^{18,19} Analogues of nivolumab⁵⁶ and pembrolizumab⁵⁷ refer to antibodies having identical amino

acid sequences to the commercial products Opdivo® and Keytruda® and were generated by cloning of synthesized genes based on published sequences and subsequent expression in mammalian cells.

Binding to human, cynomolgus and mouse PD1

Binding to the extracellular domain (ECD) of human PD1 (PD1-H5257, Acro Biosystems), cynomolgus PD1 (PD1-C5254), or mouse PD1 (PD1-M5259) immobilized onto a 96-well microtiter plate was detected with a horseradish peroxidase (HRP)-labeled anti-lambda light chain detection antibody (Abcam, ab9007) and a chromogenic HRP substrate (TMB). GraphPad Prism software was used to calculate EC50 values using a 4-parameter logistics nonlinear regression model.

Cellular PD-L1 and PD-L2 blocking assay

The ability to block the interaction of PD1 with its ligands PD-L1 or PD-L2 was assessed using PD1/PD-L1 and PD1/PD-L2 cellular blocking reporter assays performed according to the manufacturer's instructions (Promega). In brief, PD1-expressing reporter cells and PD-L1/2-expressing target cells were thawed according to the technical manual and co-cultured in a 384-well plate with the different PD1 antibodies and antibody controls at an effector-to-target cell ratio of 1:1.25 for 24 h at 37°C/5% CO₂. Following incubation, culture plates were cooled at RT for 15 min and a Bio-Glo™ reagent was added to all wells prior to measuring the level of luminescence. Antibody blocking was assessed by normalizing luminescence of antibody-treated cells to untreated cells.

In vitro functional evaluation

Human PBMCs used for *in vitro* assays were isolated by density gradient centrifugation using Lymphoprep™ solution (Stemcell technologies) from buffy coats obtained from healthy blood donors (Blood Bank, University Hospital Copenhagen, Denmark). PBMCs from cynomolgus monkeys were obtained from Worldwide Primates Inc. Isolated spleen cells from C57B1/6 mice were used for murine *in vitro* assays.

The humanized antibody repertoire was initially screened for functional activity in the SEB (*Staphylococcus* Enterotoxin B) whole blood assay. Whole blood was obtained from healthy volunteers and SEB was added at a final concentration of 1 µg/ml. After 2 days of culture, supernatants were harvested, and IL-2 levels determined by ELISA. Functional activity of the antibodies was validated in a one-way MLR assay. Dendritic cells were differentiated from CD14⁺ monocytes isolated from PBMCs by culturing for 6 days with 20 ng/ml granulocyte-macrophage-colony-stimulating factor and 20 ng/ml IL-4, and then mixed at a 1:10 ratio with CD4⁺ T-cells isolated from PBMCs from healthy blood donors. After 5 days of co-culture, supernatants were harvested and IFN-γ levels were determined using the Mesoscale electrochemiluminescence cytokine assay. During the last 5 h of the MLR assay, cell samples intended for intracellular cytokine staining were treated with Brefeldin A (Biolegend).

Antibodies and flow cytometry

The following human antibodies were used: Anti-CD4-PerCP Cy 5.5 (clone SK3), anti-IFN- γ -BV421 (4.S.B3), anti-CD8 PE-Cy7 (RPA-T8), anti-CD3 APC-H7 (SK7), anti-HLA-DR PerCP-Cy5.5 (G46-6) and anti-Ki-67-BV421 (B56) were purchased from BD, anti-TNF α -APC (MAb11) was purchased from eBioscience, and anti-CD25-APC/BV421 (V T-072) was purchased from Biolegend.

For flow cytometric analysis of tumor-infiltrating lymphocytes, tumors were harvested and processed into single cell suspensions using a tumor cell isolation kit and the GentleMACS Octo Dissociator (Miltenyi Biotec) according to the manufacturer's descriptions. One million cells were pre-incubated with an Fc-block (Miltenyi Biotec), washed and stained for cell surface markers according to standard procedures. Cells from MLR experiments were stained for cell surface markers using an Fc-block (BD Pharmingen) together with a -ZombieAquaTM Fixable Viability dye (Biolegend). For intracellular (cytoplasmic) staining, cells were fixed and permeabilized using IC Fixation/permeabilization Buffer (eBioscience). For staining of the nuclear protein Ki67, a Foxp3/Transcription Factor Staining Buffer Set (eBioscience) was used for fixation/permeabilization. Cells were acquired on a BD FACSCelesta or a FACSVerse flow cytometer (BD Biosciences). Data were collected using either BD FACS Diva v8.0.1.1 or BD FACSuite Software (v1.6) and further analyzed with FlowJo v10.4.2 (Tree Star Inc.) and GraphPad Prism v5.04 (GraphPad Software Inc.). Samples were analyzed by gating on viable cells followed by exclusion of duplets. All results show fluorescence on a bi-exponential scale.

In vivo models

To generate syngeneic tumor models, Sa1N, CT26, ASB-XIV, and MC38 cells were inoculated subcutaneously (s.c.) into the flank of 7–9-week-old A/J (Envigo), BALB/c (Janvier Labs), or C57Bl/6 (Janvier Labs) mice. To generate PBMC, humanized mice engrafted with A375 xenografts, 8–10 weeks old NOG mice from Taconic were inoculated s.c. into the flank with A375 tumor cells on day 0 and received PBMC intraperitoneally (i.p.) on study day 1 or 2. To generate fully humanized mice, female huNSG-SGM3 mice were engrafted with human CD34⁺ cells and study animals were selected that had >25% human CD45⁺ cells in the peripheral blood 10–11 weeks post engraftment. Cohorts of huNSG-SGM3 mice engrafted with CD34⁺ cells from three different donors were used. Two to four animals per donor were included in each treatment group. huNSG-SGM3 mice were implanted s.c. on the right flank with patient-derived xenograft (PDX) lung tumor tissues at passage P4. The PDX study in huNSG-SGM3 mice was conducted by the Jackson Laboratory (Sacramento, CA, USA). In all *in vivo* experiments, mice were monitored daily, and tumors measured two or three times weekly by caliper. Tumor volume was calculated using the formula: $0.5 \times \text{length} \times \text{width} \times \text{width}$. At a predetermined tumor size, mice were randomized into groups and treatment initiated. For PBMC humanized NOG mice, treatment was initiated on the same day as

PBMC inoculation. Antibodies were administered at 10 mg/kg total antibody three times weekly by i.p. injection for a total of six doses, except for the PDX study in huNSG-SGM3 mice where antibodies were administered at 10 mg/kg once followed by 5 mg/kg every 5 days. For depletion of CD4 or CD8 T cells, two days prior to tumor inoculation and hereafter twice weekly, mice received vehicle buffer or 200 μg of either CD4 (GK1.5, Bioxcell) or CD8 (YTS 169.4, Bioxcell) depletion antibody. All *in vivo* studies were performed in accordance with applicable laws or regulations relating to the care and use of laboratory animals.

Surface plasmon resonance affinity measurements

The Kinetic binding analysis was performed by SPR using a Continuous Flow Microspotter (CFM, Wasatch Microfluidics, US) combined with an IBIS MX96 SPR instrument (IBIS Technologies, The Netherlands). SPR imaging analysis was performed on anti-hu-IgG Fc SensEye[®] SPR sensors (Ssens BV, The Netherlands). Anti-PD1 antibodies (0.375 $\mu\text{g}/\text{ml}$) were spotted on the sensor for 15 min using the CFM module, followed chip transfer to the IBIS MX96 biosensor for SPR measurements. Kinetic analysis was performed by applying a so-called kinetic titration series,⁵⁸ where monomeric human, mouse or cynomolgus PD1 ECDs (Acro Biosystems) were injected in increasing concentrations without application of surface regeneration steps after each antigen injection. Antigen association was performed for 15 min, and antigen dissociation was performed for 60 min. The recorded binding responses were fitted to a simple Langmuir 1:1 binding model with Scrubber 2 software for calculation of the on-rate (k_{on} or k_a), off-rate (k_{off} or k_d), and affinity (KD) constants.

Epitope mapping with PD1 mutagenesis

A molecular model of human PD1 was built by combining structural information from the crystal structure of human PD1/human PD-L1 complex determined at 2.45 Å resolution (PDB:4ZQK) and an NMR structure of unliganded human PD1 (PDB:2M2D). The structure PDB:4ZQK was used as the basis for the model with the missing C'D loop and c-terminal part of PD1 provided from the NMR structure. Next, surface exposed amino acid residues were identified, and 88 individual alanine substitutions were introduced on surface-exposed residues on human PD1 (alanine scanning) spanning position 21 to position 167. To map linear antibody epitopes in the context of the native human PD1 structure, 23 chimeric proteins were generated where 10 amino acids in the human PD1 sequence were sequentially exchanged to the chicken sequence in segments that overlapped by five amino acids. Sequence exchanges were performed in the extracellular domain of human PD1 spanning amino acids 31–146, since the chicken PD1 protein sequence outside this segment did not show high sequence identity. All designed constructs were prepared by gene synthesis and used for transient expression in an expression construct allowing fusion of PD1 with human IgG1 Fc. Antibody binding to the mutagenized PD1 constructs was analyzed by SPR by immobilizing PD1-Fc fusion protein culture supernatants, followed by injection with

monomeric antigen-binding fragments (Fabs) of PD1 antibodies in increasing concentrations from 1 nM to 50 nM. Fab association was performed for 15 min, and antigen dissociation was performed for 30 min. The KDs were calculated as described for the affinity measurements above. Binding was expressed as the ratio KD mutant/KD WT, and a cut-off of at least 5 KDs was set for detecting significant binding differences of Fabs to the different PD1 mutants. The chicken antibody mAb7 served as a positive control for PD1 mutant expression and folding, since this antibody bound to a different location on PD1 compared to other tested antibodies and outside of the tested segment. In total, 4 of the 23 chicken/human chimeric constructs (constructs 51–70, 71–80, 91–100, 96–105) did not bind any of the tested antibodies, suggesting that the mutations caused major conformational perturbations. These four PD1 constructs were not included in the analysis.

Bioinformatics and statistical analyses

All biological sequence analyses were performed using CLC MainWorkbench (Qiagen) with a custom-developed antibody analysis plugin tool. Protein structure modeling and coloring was done using Pymol (DeLano Scientific). FACS data in Figure 4D were analyzed by one-way ANOVA with a Tukey multiple comparisons test to determine significant differences among groups. Two-way ANOVA with Bonferroni's multiple comparisons test was applied to compare tumor volumes at each time-point between treatment groups.



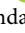






Acknowledgments

The authors wish to thank Mikkel Ammentorp Storm for assistance with protein structure modeling.

Disclosure statement

All listed authors are current or former employees of Symphogen A/S.

ORCID

Torben Gjetting  <http://orcid.org/0000-0003-1720-474X>
 Camilla Fröhlich  <http://orcid.org/0000-0001-8391-2416>
 Michael M Grandal  <http://orcid.org/0000-0001-5434-9978>
 Nikolaj Dietrich  <http://orcid.org/0000-0002-3477-0922>
 Magnus Strandh  <http://orcid.org/0000-0002-6878-1566>
 Johan Lantto  <http://orcid.org/0000-0002-8650-7157>
 Thomas Bouquin  <http://orcid.org/0000-0002-9597-8137>
 Mikkel W Pedersen  <http://orcid.org/0000-0001-5711-9051>
 Klaus Koefoed  <http://orcid.org/0000-0001-8945-3791>

References

- Carter PJ, Lazar GA. Next generation antibody drugs: pursuit of the 'high-hanging fruit'. *Nat Rev Drug Discov.* 2018;17(3):197–223. doi:10.1038/nrd.2017.227. PMID: 29192287.
- William R. Strohl Current progress in innovative engineered antibodies. *Protein Cell.* 2018;9(1):86–120. doi:10.1007/s13238-017-0457-8. PMID: 28822103.
- Green LL. Transgenic mouse strains as platforms for the successful discovery and development of human therapeutic monoclonal antibodies. *Curr Drug Discov Technol.* 2014;11(1):74–84. PMID: 23978036.
- Frenzel A, Schirrmann T, Hust M. Phage display-derived human antibodies in clinical development and therapy. *MAbs.* 2016;8(7):1177–94. doi:10.1080/19420862.2016.1212149. PMID: 27416017.
- International Chicken Genome Sequencing Consortium. Sequence and comparative analysis of the chicken genome provide unique perspectives on vertebrate evolution. *Nature.* 2004;432(7018):695–716. Erratum in: *Nature.* 2005 433(7027):777. doi:10.1038/nature03154. PMID: 15592404.
- Hedges SB, Marin J, Suleski M, Paymer M, Kumar S. Tree of life reveals clock-like speciation and diversification. *Mol Biol Evol.* 2015;32(4):835–45. doi:10.1093/molbev/msv037. PMID: 25739733 PMID: PMC4379413.
- Parvari R1, Avivi A, Lentner F, Ziv E, Tel-Or S, Burstein Y, Schechter I. Chicken immunoglobulin gamma-heavy chains: limited VH gene repertoire, combinatorial diversification by D gene segments and evolution of the heavy chain locus. *Embo J.* 1988;7(3):739–44. PMID: 3135182 PMID: PMC454383.
- Reynaud CA, Dahan A, Anquez V, Weill JC. Somatic hyperconversion diversifies the single Vh gene of the chicken with a high incidence in the D region. *Cell.* 1989;59(1):171–83. PMID: 2507167.
- Ratcliffe MJ. Antibodies, immunoglobulin genes and the bursa of Fabricius in chicken B cell development. *Dev Comp Immunol.* 2006;30(1–2):101–18. doi:10.1016/j.dci.2005.06.018. PMID: 16139886.
- Wu L, Oficjalska K, Lambert M, Fennell BJ, Darmanin-Sheehan A, Ní Shúilleabháin D, Autin B, Cummins E, Tchistiakova L, Bloom L, et al. Fundamental characteristics of the immunoglobulin VH repertoire of chickens in comparison with those of humans, mice, and camelids. *J Immunol.* 2012;188(1):322–33. doi:10.4049/jimmunol.1102466. PMID: 22131336.
- Abdiche YN, Harriman R, Deng X, Yeung YA, Miles A, Morishige W, Boustany L, Zhu L, Izquierdo SM, Harriman W. Assessing kinetic and epitopic diversity across orthogonal monoclonal antibody generation platforms. *MAbs.* 2016;8(2):264–77. doi:10.1080/19420862.2015.1118596. PMID: 26652308.
- Meijer PJ, Andersen PS, Haahr Hansen M, Steinaa L, Jensen A, Lantto J, Oleksiewicz MB, Tengbjerg K, Poulsen TR, Coljee VW, et al. Isolation of human antibody repertoires with preservation of the natural heavy and light chain pairing. *J Mol Biol.* 2006;358(3):764–72. doi:10.1016/j.jmb.2006.02.040. PMID: 16563430.
- Ishida Y, Agata Y, Shibahara K, Honjo T. Induced expression of PD-1, a novel member of the immunoglobulin gene superfamily, upon programmed cell death. *Embo J.* 1992;11(11):3887–95. PMID: 1396582 PMID: PMC556898.
- Agata Y, Kawasaki A, Nishimura H, Ishida Y, Tsubata T, Yagita H, Honjo T. Expression of the PD-1 antigen on the surface of stimulated mouse T and B lymphocytes. *Int Int Immunol.* 1996;8(5):765–72. PMID: 8671665.
- Pardoll DM. The blockade of immune checkpoints in cancer immunotherapy. *Nat Rev Cancer.* 2012;12(4):252–64. doi:10.1038/nrc3239. PMID: 22437870.
- Okazaki T, Chikuma S, Iwai Y, Fagarasan S, Honjo T. A rheostat for immune responses: the unique properties of PD-1 and their advantages for clinical application. *Nat Immunol.* 2013 Dec;14(12):1212–18. doi:10.1038/ni.2762. PMID: 24240160.
- Gong J, Chehrizi-Raffle A, Reddi S, Salgia R. Development of PD-1 and PD-L1 inhibitors as a form of cancer immunotherapy: a comprehensive review of registration trials and future considerations. *J Immunother Cancer.* 2018;6:8. doi:10.1186/s40425-018-0316-z. PMID: PMC5778665 PMID: 29357948.
- Hezareh M, Hessel AJ, Jensen RC, van de Winkel JG, Parren PW. Effector function activities of a panel of mutants of a broadly neutralizing antibody against human immunodeficiency virus type 1. *J Virol.* 2001;75(24):12161–68. doi:10.1128/JVI.75.24.12161-12168.2001. PMID: 11711607.
- Hessel AJ, Hangartner L, Hunter M, Havenith CE, Beurskens FJ, Bakker JM, Lanigan CM, Landucci G, Forthal DN, Parren PW, et al. Fc receptor but not complement binding is important in

- antibody protection against HIV. *Nature*. 2007;449(7158):101–04. doi:10.1038/nature06106. PMID: 17805298.
20. Sievers F, Wilm A, Dineen D, Gibson TJ, Karplus K, Li W, Lopez R, McWilliam H, Remmert M, Söding J, et al. Scalable generation of high-quality protein multiple sequence alignments using Clustal Omega. *Mol Syst Biol*. 2011;7:539. doi:10.1038/msb.2011.75. PMID: 21988835.
 21. Köntzer JD, Pramanick S, Pan Q, Augustin R, Bandholtz S, Harriman W, Izquierdo S. Generation of a highly diverse panel of antagonistic chicken monoclonal antibodies against the GIP receptor. *MAbs*. 2017;9(3):536–49. doi:10.1080/19420862.2016.1276683. PMID: 28055305.
 22. Shi B, Ma L, He X, Wang X, Wang P, Zhou L, Yao X. Comparative analysis of human and mouse immunoglobulin variable heavy regions from IMGT/LIGM-DB with IMGT/HighV-QUEST. *Theor Biol Med Model*. 2014;11:30. doi:10.1186/1742-4682-11-30. PMID: 24992938.
 23. Buchanan A, Clementel V, Woods R, Harn N, Bowen MA, Mo W, Popovic B, Bishop SM, Dall'Acqua W, Minter R, et al. Engineering a therapeutic IgG molecule to address cysteinylolation, aggregation and enhance thermal stability and expression. *MAbs*. 2013;5(2):255–62. doi:10.4161/mabs.23392. PMID: 23412563.
 24. Jarasch A, Koll H, Regula JT, Bader M, Papadimitriou A, Kettenberger H. Developability assessment during the selection of novel therapeutic antibodies. *J Pharm Sci*. 2015;104(6):1885–98. doi:10.1002/jps.24430. PMID: 25821140.
 25. Jones PT, Dear PH, Foote J, Neuberger MS, Winter G. Replacing the complementarity-determining regions in a human antibody with those from a mouse. *Nature*. 1986;321(6069):522–25. doi:10.1038/321522a0. PMID: 3713831.
 26. Foote J, Winter G. Antibody framework residues affecting the conformation of the hypervariable loops. *J Mol Biol*. 1992;224:487–99. doi:10.1016/0022-2836(92)91010-M. PMID: 1560463.
 27. Sela-Culang I, Kunik V, Ofran Y. The structural basis of antibody-antigen recognition. *Front Immunol*. 2013;4:302. doi:10.3389/fimmu.2013.00302. PMID: 24115948.
 28. Townsend S, Fennell BJ, Apgar JR, Lambert M, McDonnell B, Grant J, Wade J, Franklin E, Foy N, Ni Shúilleabháin D, et al. Augmented binary substitution: single-pass CDR germ-lining and stabilization of therapeutic antibodies. *Proc Natl Acad Sci U S A*. 2015;112(50):15354–59. doi:10.1073/pnas.1510944112. PMID: 26621728.
 29. Lin DY, Tanaka Y, Iwasaki M, Gittis AG, Su HP, Mikami B, Okazaki T, Honjo T, Minato N, Garboczi DN. The PD-1/PD-L1 complex resembles the antigen-binding Fv domains of antibodies and T cell receptors. *Proc Natl Acad Sci U S A*. 2008;105(8):3011–16. doi:10.1073/pnas.0712278105. PMID: 18287011.
 30. Zak KM, Kitel R, Przetocka S, Golik P, Guzik K, Musielak B, Dömling A, Dubin G, Holak TA. Structure of the complex of human programmed death 1, PD1, and its ligand PD-L1. *Structure*. 2015;23(12):2341–48. doi:10.1016/j.str.2015.09.010. PMID: 26602187.
 31. Tan S, Zhang H, Chai Y, Song H, Tong Z, Wang Q, Qi J, Wong G, Zhu X, Liu WJ, et al. An unexpected N-terminal loop in PD1 dominates binding by nivolumab. *Nat Commun*. 2017;8:14369. doi:10.1038/ncomms14369. PMID: 28165004.
 32. Carroll SB, Stollar BD. Antibodies to calf thymus RNA polymerase II from egg yolks of immunized hens. *J Biol Chem*. 1983 Jan 10;258(1):24–26. PMID: 6336747.
 33. Gassmann M, Thömmes P, Weiser T, Hübscher U. Efficient production of chicken egg yolk antibodies against a conserved mammalian protein. *FASEB J*. 1990;4(8):2528–32. PMID: 1970792.
 34. Tucker DF, Sullivan JT, Mattia KA, Fisher CR, Barnes T, Mabila MN, Wilf R, Sulli C, Pitts M, Payne RJ, et al. Isolation of state-dependent monoclonal antibodies against the 12-transmembrane domain glucose transporter 4 using virus-like particles. *Proc Natl Acad Sci U S A*. 2018;115(22):E4990–E4999. doi:10.1073/pnas.1716788115. PMID: 29769329.
 35. Li D, Xu J, Wang Z, Gong Z, Liu J, Zheng Y, Li J. Epitope mapping reveals the binding mechanism of a functional antibody cross-reactive to both human and murine programmed death 1. *MAbs*. 2017;9(4):628–37. doi:10.1080/19420862.2017.1296612. PMID: 28300475.
 36. Andris-Widhopf J, Rader C, Steinberger P, Fuller R, Barbas CF. Methods for the generation of chicken monoclonal antibody fragments by phage display. *J Immunol Methods*. 2000;242(1–2):159–81. PMID: 10986398.
 37. Tsurushita N, Park M, Pakabunto K, Ong K, Avdalovic A, Fu H, Jia A, Vásquez M, Kumar S. Humanization of a chicken anti-IL-12 monoclonal antibody. *J Immunol Methods*. 2004;295(1–2):9–19. doi:10.1016/j.jim.2004.08.018.
 38. Ching KH, Collarini EJ, Abdiche YN, Bedinger D, Pedersen D, Izquierdo S, Harriman R, Zhu L, Etches RJ, van de Lavoie MC, et al. Chickens with humanized immunoglobulin genes generate antibodies with high affinity and broad epitope coverage to conserved targets. *MAbs*. 2018;10(1):71–80. doi:10.1080/19420862.2017.1386825. PMID: 29035625.
 39. Sorouri M, Fitzsimmons SP, Aydianian AG, Bennett S, Shapiro MA. Diversity of the antibody response to tetanus toxoid: comparison of hybridoma library to phage display library. *PLoS One*. 2014;9(9):e106699. doi:10.1371/journal.pone.0106699. PMID: 25268771.
 40. Adler AS, Bedinger D, Adams MS, Asensio MA, Edgar RC, Leong R1, Leong J, Ra M, Mj S, Sr B, et al. A natively paired antibody library yields drug leads with higher sensitivity and specificity than a randomly paired antibody library. *MAbs*. 2018;10(3):431–43. doi:10.1080/19420862.2018.1426422. PMID: 29376776.
 41. West AP Jr, Scharf L, Scheid JF, Klein F, Bjorkman PJ, Nussenzweig MC. Structural insights on the role of antibodies in HIV-1 vaccine and therapy. *Cell*. 2014;156(4):633–48. doi:10.1016/j.cell.2014.01.052. PMID: 24529371.
 42. Sok D, Le KM, Vadnais M, Saye-Francisco KL, Jardine JG, Torres JL, Berndsen ZT, Kong L, Stanfield R, Ruiz J, et al. Rapid elicitation of broadly neutralizing antibodies to HIV by immunization in cows. *Nature*. 2017;548(7665):108–11. doi:10.1038/nature23301. PMID: 28726771.
 43. Patnaik A, Kang SP, Rasco D, Papadopoulos KP, Ellassaiss-Schaap J, Beeram M, Drengler R, Chen C, Smith L, Espino G, et al. Phase I study of pembrolizumab (MK-3475; anti-PD-1 monoclonal antibody) in patients with advanced solid tumors. *Clin Cancer Res*. 2015;21(19):4286–93. doi:10.1158/1078-0432.CCR-14-2607. PMID: 25977344.
 44. Lindauer A, Valiathan CR, Mehta K, Sriram V, de Greef R, Ellassaiss-Schaap J, de Alwis DP. Translational pharmacokinetic/pharmacodynamic modeling of tumor growth inhibition supports dose-range selection of the anti-PD-1 antibody pembrolizumab. *CPT Pharmacometrics Syst Pharmacol*. 2017;1:11–20. doi:10.1002/psp4.12130. PMID: 27863176.
 45. Zemlin M, Klinger M, Link J, Zemlin C, Bauer K, Engler JA, Schroeder HW Jr, Kirkham PM. Expressed murine and human CDR-H3 intervals of equal length exhibit distinct repertoires that differ in their amino acid composition and predicted range of structures. *J Mol Biol*. 2003;334(4):733–49. PMID: 14636599.
 46. Lantto J, Haahr Hansen M, Rasmussen SK, Steinaa L, Poulsen TR, Duggan J, Dennis M, Naylor I, Easterbrook L, Bregenholt S, et al. Capturing the natural diversity of the human antibody response against vaccinia virus. *J Virol*. 2011;85(4):1820–33. doi:10.1128/JVI.02127-10. PMID: 21147924.
 47. Akbari S1, Pirbodaghi T. A droplet-based heterogeneous immunoassay for screening single cells secreting antigen-specific antibodies. *Lab Chip*. 2014;14(17):3275–80. doi:10.1039/c4lc00082j. PMID: 24989431.
 48. DeKosky BJ, Kojima T, Rodin A, Charab W, Ippolito GC, Ellington AD, Georgiou G. In-depth determination and analysis of the human paired heavy- and light-chain antibody repertoire. *Nat Med*. 2015 Jan;21(1):86–91. doi:10.1038/nm.3743. PMID: 25501908.
 49. Adler AS, Mizrahi RA, Spindler MJ, Adams MS, Asensio MA, Edgar RC, Leong J, Leong R, Johnson DS. Rare, high-affinity mouse anti-PD-1 antibodies that function in checkpoint blockade, discovered using microfluidics and molecular genomics. *MAbs*.

- 2017a;9(8):1270–81. doi:10.1080/19420862.2017.1371386. PMID: 28846506.
50. Adler AS, Mizrahi RA, Spindler MJ, Adams MS, Asensio MA, Edgar RC, Leong J, Leong R, Roalfe L, White R, et al. Rare, high-affinity anti-pathogen antibodies from human repertoires, discovered using microfluidics and molecular genomics. *MAbs*. 2017b;9(8):1282–96. doi:10.1080/19420862.2017.1371383. PMID: 28846502.
51. Wang B, DeKosky BJ, Timm MR, Lee J, Normandin E, Misasi J, Kong R, McDaniel JR, Delidakis G, Leigh KE, et al. Functional interrogation and mining of natively paired human VH:VL antibody repertoires. *Nat Biotechnol*. 2018;36(2):152–55. doi:10.1038/nbt.4052. PMID: 29309060.
52. Meijer PJ, Nielsen LS, Lantto J, Jensen A. Human antibody repertoires. *Methods Mol Biol*. 2009;525:261–77. doi:10.1007/978-1-59745-554-1_13. PMID: 19252857.
53. Baldi P, Chauvin Y, Hunkapiller T, McClure MA. Hidden Markov models of biological primary sequence information. *Proc Natl Acad Sci U S A*. 1994;91(3):1059–63. PMID: 8302831.
54. Koefoed K, Steinaa L, Søderberg JN, Kjær I, Jacobsen HJ, Meijer PJ, Haurum JS, Jensen A, Kragh M, Andersen PS, et al. Rational identification of an optimal antibody mixture for targeting the epidermal growth factor receptor. *MAbs*. 2011;3(6):584–95. doi:10.4161/mabs.3.6.17955. PMID: 22123060.
55. Lefranc MP, Giudicelli V, Ginestoux C, Bodmer J, Müller W, Bontrop R, Lemaitre M, Malik A, Barbié V, Chaume D. IMGT, the international ImmunoGeneTics database. *Nucleic Acids Res*. 1999;27(1):209–12. PMID: 9847182.
56. Rajan A, Kim C, Heery CR, Guha U, Gulley JL. Nivolumab, anti-programmed death-1 (PD-1) monoclonal antibody immunotherapy: role in advanced cancers. *Hum Vaccin Immunother*. 2016;12(9):2219–31. doi:10.1080/21645515.2016.1175694. PMID: 27135835.
57. Kwok G, Yau TC, Chiu JW, Tse E, Kwong YL. Pembrolizumab (Keytruda). *Hum Vaccin Immunother*. 2016;12(11):2777–89. doi:10.1080/21645515.2016.1199310. PMID: 27398650.
58. Karlsson R. Biosensor binding data and its applicability to the determination of active concentration. *Biophys Rev*. 2016;8(4):347–58. doi:10.1007/s12551-016-0219-5. PMID: 28510014.